A new impedance sensor for industrial applications

Jean-Christophe Le Roux, Marc Pachebat, Jean-Pierre Dalmont

A new impedance sensor for industrial applications

J.C. Le Roux[a], M. Pachebat[b] and J.-P. Dalmont[c]

[a]CTTM, 20, rue Thales de Milet, 72000 Le Mans, France
[b]LMA, CNRS, UPR 7051, Aix-Marseille Univ, Centrale Marseille, 13402 Marseille, France
[c]Laboratoire d'acoustique de l'université du Maine, Bât. IAM - UFR Sciences Avenue Olivier Messiaen 72085 Le Mans Cedex 9
jcleroux@cttm-lemans.com

Some years ago, the LAUM, together with the CTTM developed a first impedance sensor based on a controlled volume velocity source. The impedance of a measured system was easily and accurately obtained from 20 to 5000 Hz. Due to the low level of the generated volume velocity, this sensor is mainly devoted to laboratory studies (musical acoustics, porous material characterization,…). For this measurement principle to be applied to engineering topics, a new device is conceived, using a recently developed electrodynamic transducer. In particular, leakages between its front and back sides should be reduced to a minimum, and mechanical resonances must be rejected out of the frequency range of interest. To illustrate the capabilities of this new impedance sensor, the characterization and tuning of a loudspeaker bass reflex enclosure is performed. The sensor measures the low frequency acoustic impedance of the enclosure seen from the loudspeaker location. The measured impedance is then compared with a lumped element model. The analysis of the impedance magnitude is used to cancel the acoustic resonances inside the volume and to check the correct tuning of the bass reflex system.

1 Introduction

A new setup for the measurement of acoustic impedance is presented. The principle is based on a controlled volume velocity source [1,2,3]. This sensor uses a new loudspeaker technology featuring suited mechanical and acoustical properties. In comparison with a previous sensor [2], the new one is mainly devoted to the low frequency measurement of larges equipments. As an example of possible industrial application, the new sensor has been used for the characterization and the control of a loudspeaker column enclosure. Comparisons with simulations performed with lumped element model are also performed.

2 Principle

The proposed impedance measurement setup uses a perfect rigid piston as a source. This piston is loaded on its back to a closed cavity and is connected to the front to the measured device (see figure 1). The pressures p_2 at the output of the sensor and p_1 in the back cavity are measured by two microphones. At first order, the pressure p_1 is proportional to the volume velocity U delivered by the rigid piston. The impedance $Z_{sensor} = p_2 / U$ is thus at first order proportional to the ratio between the pressure of the two microphones written:

$$\frac{p_2}{p_1} = -jC\omega Z_{sensor} \qquad (1)$$

where $C = V / \rho c^2$ is the acoustic compliance of the back cavity of volume V, with ρ the air density and c the speed of sound.

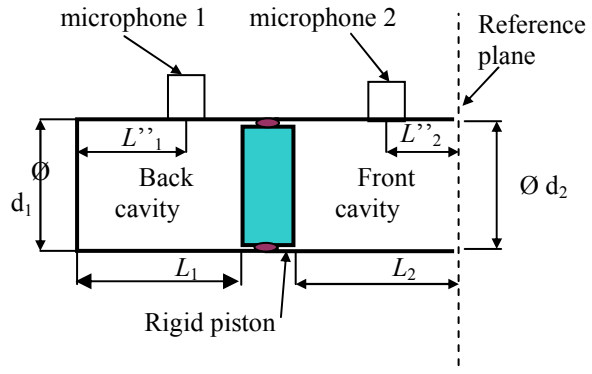

Fig.1 Schematic drawing of the impedance measurement sensor and notations

In practice equation (1) is only valid for low frequencies. Moreover, it is necessary to take into account the relative sensitivity of the two microphones, since the quantity actually measured is $H_{21} = p_2 s_2 / p_1 s_1$ with s_1, s_2 the respective sensitivities of microphones 1 and 2. It is also possible to calculate more precisely the expression of the impedance by taking into account the geometrical dimensions of the sensor:

$$Z_{sensor} = \frac{H_{21}/K - \beta}{1 - \delta H_{21}/K} \quad , \qquad (2)$$

with

$$K = -j\frac{1}{Z_{c1}}\frac{s_2}{s_1}\frac{\sin(kL_1)}{\cos(kL_1'')}\frac{\cos(kL_2'')}{\cos(kL_2)} \quad , \qquad (3)$$

$$\beta = jZ_{c2}\tan(kL_2'') \quad , \qquad (4)$$

$$\delta = j\tan(kL_2)/Z_{c2} \quad . \qquad (5)$$

Lengths L_1, L_2, L''_1 et L''_2 are the dimensions related to the sensor geometry and to the position of the microphones as indicated on figure (1). $Z_{c1} = \rho c / S_1$ and $Z_{c2} = \rho c / S_2$ are the respective characteristic impedances of the front and back cavities ($S_1 = \pi d_1^{\,2} / 4$ is the cross section of the back cavity with d_1 its diameter and the same for the front cavity).

In a theoretical sensor, only the relative sensitivity of the microphones is unknown, geometrical quantities being accurately assessed with a calibre. In practice, the shape of the sensor can be slightly different than the theoretical one and the geometrical quantities cannot be measured directly. Thus a complete "factory calibration procedure" of the sensor has been successfully developed, based on the measurement of three non resonant acoustics loads [4,6]. In a general use, only a relative calibration is requested and can be easilly done by loading the sensor head with an infinite impedance (i.e a rigid plate).

The complete calibration of the sensor is essential to perform accurate measurements at mid and high frequencies. For low frequencies applications, a simplified calibration procedure is used. By loading the sensor head with an infinite impedance, the measured transfer function expression reduce to $H_{21}^{\infty} = K / \delta$. Then, equation (2) can be rewritten as follows :

$$Z_{sensor} = \frac{1}{\delta}\frac{H_{21}/H_{21}^{\infty} - \delta\beta}{1 - H_{21}/H_{21}^{\infty}} \quad . \qquad (6)$$

Knowing the dimensions L_2 and L''_2 from direct measurement of the sensor geometry, the unknown impedance is determined by the two transfer functions H_{21}^{∞} and H_{21}.

3 Description of the new impedance sensor

The core of the impedance sensor is the use of an innovative electrodynamic transducer that exhibits the following crucial characteristics:

- the membrane behaves like a perfect rigid piston up to high frequencies,
- there are no leakages between the front and the rear sides of the membrane.

Without these two characteristics, the generated volume velocity couldn't be accurately assessed and then the sensor wouldn't work properly. It's the reason why the previous impedance sensor design made use of a small piezoelectric bender instead of a commercial loudspeaker as involved in an early design [1].

The impedance sensor manufactured at CTTM is shown in figure 2. Two very stable electret microphones with dedicated conditioning are used to measure back and front pressures. As the sensitivity ratio is part of the calibration, there is no need of high quality condenser microphones. Moreover, the calibration principle that does not require to unmount the microphone provides a important accuracy gain compared to standard two microphones method.

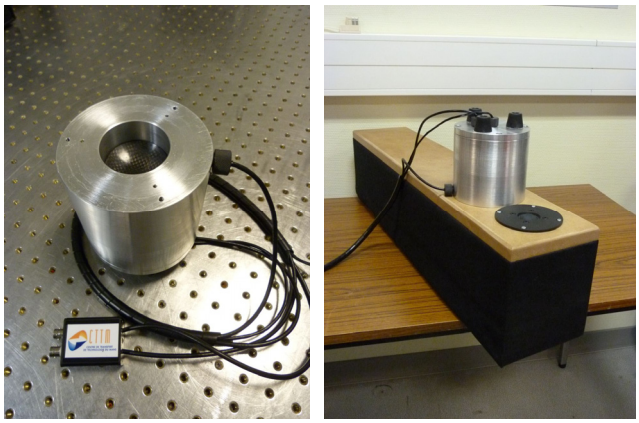

Fig.2 View of the impedance sensor and its application to loudspeaker enclosure design

4 Studied setup

To illustrate the interest of an impedance sensor, a previous paper dealt with the investigation of a complexe resonant load [1]. Here we illustrate the increase in accuracy gained over the last decade by considering the case of a loudspeaker column enclosure (its optimisation is however not the topic of this presentation). It is well known that, due to its important longitudinal dimension, the drawback of such an enclosures is that it features acoustical resonances at mid frequency [7,8]. This has a major (an undesirable) impact on loudspeaker pressure response.

A common solution is to divide the enclosure volume by a perforated wall, thus reducing the acoustic resonances in the cavity.

Two practical questions then arise:

- How to design accurately the enclosure taking into account a perforated wall?
- Does the added perforated wall modify the tuning of the enclosure in the case of a vented box?

Four configurations are studied from the same enclosure frame: closed box, vented box and vented box with undamped or damped perforated wall (figure 3). The closed box volume is 10.6L, and the theoretical vented box Helmholtz resonance frequency is 70Hz (added lengths due to air load at the inner and outer sides of the vent are respectively 1.65cm and 2.34cm).

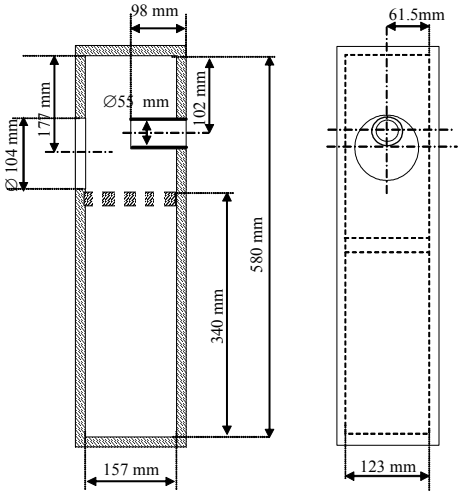

Fig.3 Description of the studied enclosures

We concentrate our work on the measurement and the simulation of the enclosure impedance as seen from the loudspeaker location. Thus, loudspeaker rear side air load is not taken into account (figure 4) [9].

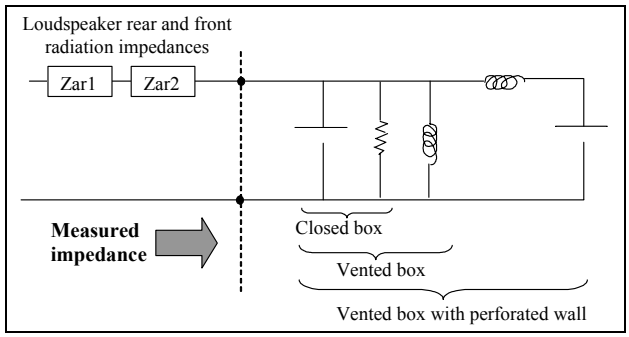

Fig.4 Current electroacoustic modelisation of enclosures

5 Simulation method

The model must describe adequately the first and second vertical resonance of the enclosure under study. This could involve a transmission line model [8], but we used an existing one, more flexible and already checked against numerous loudspeaker designs. This model uses a simple spatial discretization scheme involving lumped element approximation of the propagation inside the box.

The configuration presented on Fig. 3 is then simulated by an assembly of a sufficient number of elementary cells (fig. 5) along its vertical dimension (see fig. 6). Each elementary cell is described in terms of dipole impedances Z_i, Z_j and Z_k for its constitutive elements: the volume (index i), the radiating wall (index j) and the boundary towards its neighbors (index k, and k-1) as shown on fig 6.

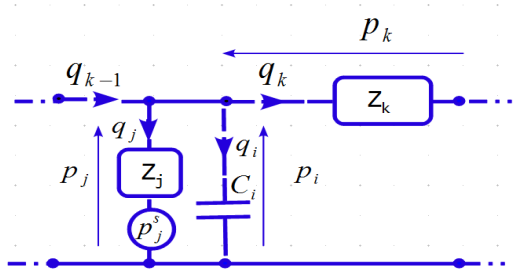

Fig.5 : equivalent circuit of an elementary cell of the discrete simulation scheme of fig. 6 (impedance analogy)

Then, for an arbitrary number of loudspeakers pressure sources located at the front p^s_j and inside the enclosure p^s_k, one can obtain the acoustic unknowns of the system (pressures p_i, p_j and p_k, and volume velocities q_i, q_j and q_k) by inverting the following algebraic system, obtained directly from the equivalent circuit of fig. 5:

$$\begin{cases} 0 = -Z_i q_i + p_i \\ p^s_j = -Z_j q_j + p_j \\ p^s_k = -Z_k q_k + p_i - p_{i+1} \\ 0 = q_i + q_j + q_k - q_{k-1} \end{cases} \quad (7)$$

In the present case, the vertical dimension of the enclosure is separated in 24 elementary cells, leading to the numerical inversion of a 95x95 matrix. This degree of discretization is able to reproduce correctly the first and second resonance of the measured impedance situated near 300 and 600 Hz (see fig. 11 and 12).

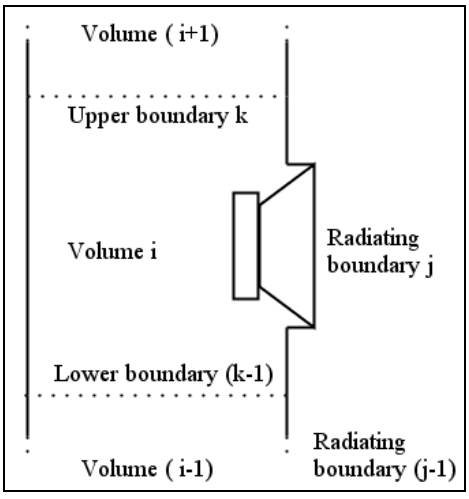

Fig.6 Schematic view of an elementary cell of the discrete simulation scheme

The impedance of the fraction of volume Z_i is described with a compliance in parallel with a thermal loss resistance estimated from the closed box measurement (fig.10). The radiating boundary impedance Z_j is described either with a classical Thiele-Small model for the loudspeaker, or a very small compliance in the other cells, where the radiating boundary is a closed wall, or by an acoustic mass equivalent to the venting including its end corrections when present.

Finally, the boundary impedance Z_k is an acoustic mass (propagation) in series with an acoustical viscous resistance of a cylindrical tube [10] estimated at the first resonance frequency of the closed box (300 Hz). When a perforated screen is present, Z_k is replaced by the expression of the impedance of a perforated screen given by Allard ([11] chap.9)

6 Results

6.1 Sensor radiation compensation

The first step of the measurement consists in compensating the sensor membrane radiation impedance ($Z_{radiation}$). This term results from the sensor surface being much smaller than the one of the enclosure, so the discontinuity at the interface leads to a local pressure (corresponding to higher-order evanescent modes) which is added to the expected 1D impedance [12]. An accurate analysis of the enclosure properties thus implies to subtract this discontinuity impedance to the measured data. As this impedance is dominated by the sensor geometry, it can be approximated as the imaginary part of a radiation impedance :

$$Z_{enclosure} = Z_{sensor} - \mathrm{Im}(Z_{radiation}) \quad (8)$$

The sensor radiation impedance should be assessed with mounting conditions as close as possible to the ones existing on the tested enclosure. The sensor is then fixed on a screen with a circular cut similar as the hole devoted to the loudspeaker mounting (see fig. 7).

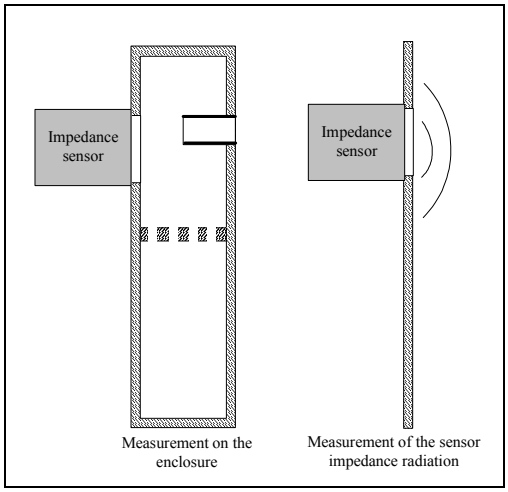

Fig.7 Set up for the measurement of $Z_{radiation}$

The figure 8 shows the measured radiation impedance. For this setup, the values are similar to the theoretical radiation impedance of a 57mm rigid piston on an infinite screen. In the followings, sensor radiation impedance is then described by its theoretical value

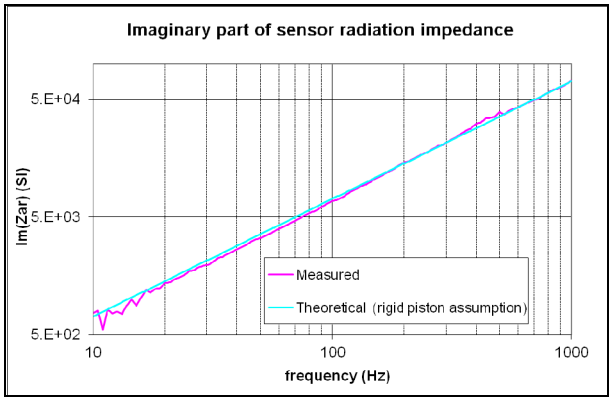

Fig.8 Imaginary part of the sensor radiation impedance

6.2 Closed and vented box

The figure 9 presents the modulus of the measured impedances for the closed and the vented enclosures. Theoretical low frequency asymptotes are also shown. The sensor give a good measurement quality, in particular at very low frequencies. It appears clearly that the measured impedances are in line with the predicted behavior of the enclosures, in particular at low frequencies. In the closed box, leakages effect can be seen below 25Hz. The figure 10 shows the corresponding admittance components. The imaginary part is similar to theoretical one of a 10.6L volume. Leakages acoustic resistance value is about 3.10^5 (SI) and the cut-off frequency is estimated to f_c=6.6Hz. Concerning the vented enclosure, the low frequency behavior is the one of the vent, and the Helmholtz resonance frequency appears as predicted at 70Hz.

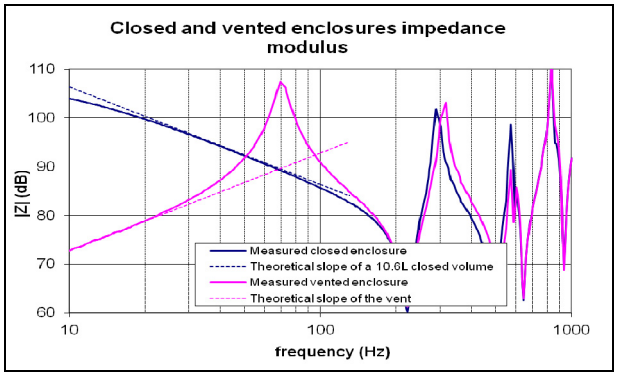

Fig.9 Acoustic impedances of closed and vented enclosures

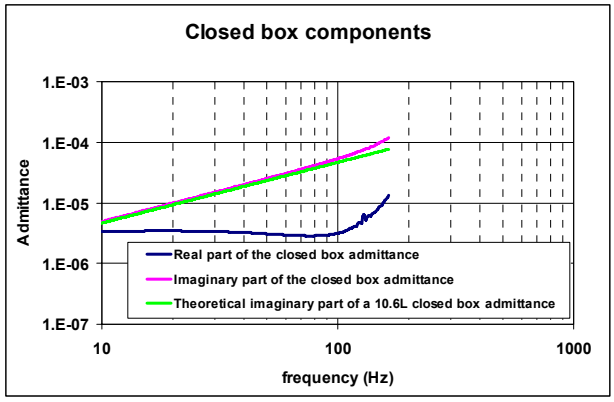

Fig.10 Closed box admittance components

Simulations have been performed accordingly to the methodology described in §5. Results are shown on fig.11 for the closed box and on fig.12 for the vented box. The enclosure behaviors are well predicted and the resonances of the cavity are in accordance with the measured data up to approximately 600 Hz. One can point out that the estimated resistance value at the low frequency limit $R=3.10^5$ (SI) given by sensor measurements (fig.10) allows the model to give a good estimation of the thermal losses inside the closed cavity. In effect, on fig.11, the predicted low frequency behavior of the model is very close to the measured one.

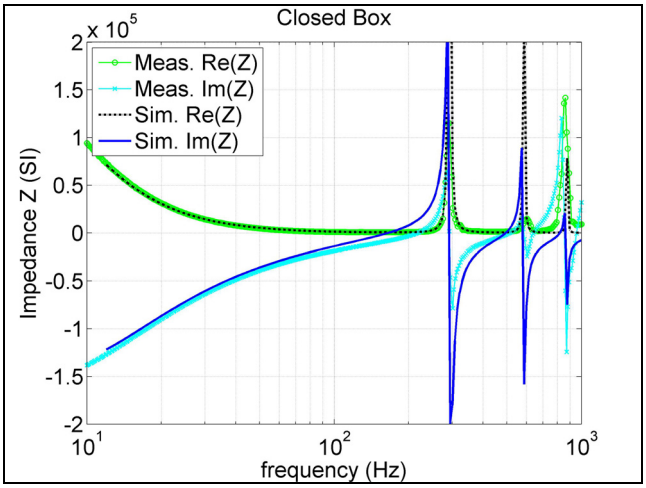

Fig.11 Closed box impedance as seen by the loudspeaker

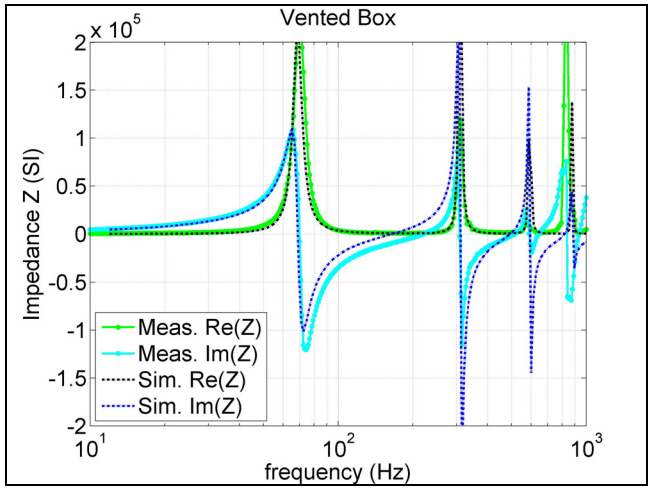

Fig.12 Vented box impedance as seen by the loudspeaker

6.3 Vented box with perforated wall

The simulation tool has then been used to give a first design of a perforated wall to be installed in the vented enclosure (see fig. 3). The Figures 13 and 14 give comparisons of measured versus simulated data for two perforated wall designs. The first one is a 4cm thick woodplate with a porosity of 20% and 1cm diameter circular holes. The second one is identical, with an added porous material layer on one side of the perforated wall.

After a slight tuning of the added length and resistance of the perforated wall, good agreement is found between measured and simulated data. In particular, the first

resonance of the vented box, at approximately 70 Hz is not significantly affected by the presence of the perforated screen.

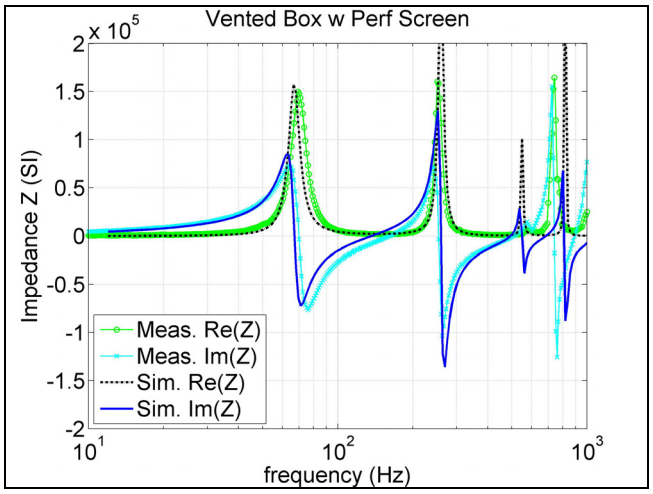

Fig.13 Vented box impedance with perforated wall design

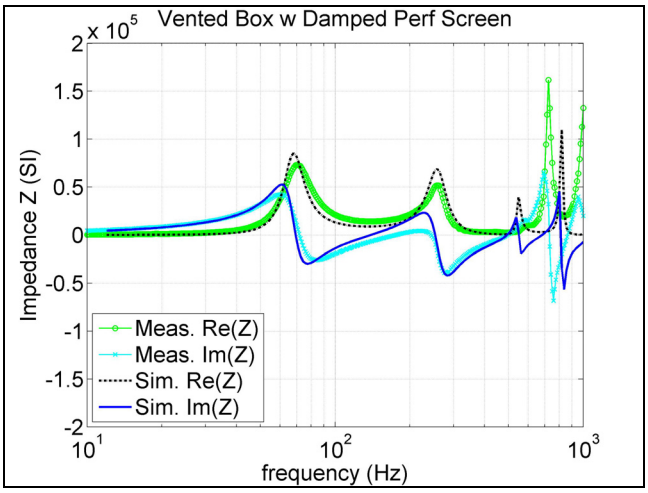

Fig.14 Vented box with damped perforated wall design,

5 Conclusion

A new impedance sensor has been presented for low frequency measurements of large equipments. For this study, a loudspeaker enclosure has been taken as an example.

The sensor is able to provide a good measurement of the enclosure impedances, in particular at very low frequencies. It then allows an accurate assessment of enclosure components: volume size and thermal losses for the closed box configuration, vent characteristics and Helmholtz resonance frequency for the bass reflex enclosure.

Sensor measurements are compared with a lumped elements model. The simulations results confirm the validity of the parameters estimated from the sensor measurements. The model is in good agreement with the data, although limited by a low frequency approach and viscous and thermal losses expressions that are constant with frequency.

The simulation software is used to propose a perforated wall to be mounted in the enclosure. The model gives a good indication on the wall design, thus limiting the number of configuration to be tested. By comparison with the impedance measured with the sensor, it is possible to tune precisely the added length and resistance of the perforated wall. Thus, the impedance sensor allows a further improvement of the perforated wall model.

The new impedance sensor proposed here, exhibit technological characteristics and calibration procedure that are adapted to “out of the lab” applications, and we illustrated how its use can give real physical insight for the design of an electroacoustic system and associated low frequency model.

This opens the way to new application of this impedance sensor to be explored like for example, orifice impedance under grazing flow, local impedance in modal acoustic room, characterization of acoustic reactive and dissipative wall treatments.

References

[1] P. Herzog, L. Desmons, E. Parizet, "Comportement électroacoustique d’un haut-parleur monté dans une portière", Congrès Français d’Acoustique (1997)

[2] J.P. Dalmont, J.C. Le Roux, “A new impedance sensor”, Congrès Français d’Acoustique, (2008)

[3] French Patent FR2933186A1

[4] J.P. Dalmont, Ph. Herzog, "Improved analysis of input impedance measurements", Proc. Institute Of Acoustics, 15(3):681-688, Southampton, 1993

[5] J.P. Dalmont: “Acoustic Impedance Measurement, Part I: a review”, J. Sound Vib. 243 (3), 427-439 (2001)

[6] P. Dickens, J. Smith and J. Wolfe: “Improved Precision in Measurements of Acoustic Impedance Spectra Using Resonance-free Calibration Loads and Controled Error Distribution”, J. Acoust. Soc. Am., 121 (3), 1471-1481 (2007)

[7] J. Backman, "A Computational Model of Transmission Line Loudspeakers", 92nd AES Convention, preprint 3326 (1992)

[8] J. Backman, "A One-Dimensional Model of Loudspeaker Enclosures", 96th AES Convention, paper 3827, (1994)

[9] M. Rossi: “Electroacoustique, Traité d’Electricité de l’Ecole Polytechnique Fédérale de Lausanne”, Volume XXI, Presses Polytechniques Romandes, Lausanne, 1986

[10] M. Bruneau : “Manuel d’acoustique fondamentale ”, Hermès Ed., 1998.

[11] Allard, J.-F., and N. Atalla : “Propagation of Sound in Porous Media: Modelling Sound Absorbing Materials”, John Wiley and Sons, 2009.

[12] J. Kergomard, A. Garcia, "Simple discontinuities in acoustic waveguides at low frequencies : critical analysis and formulae", J. Sound Vib. 114(3):465-479 (1987)